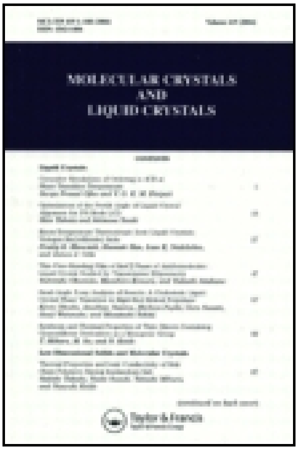

Molecular Crystals and Liquid Crystals Science and Technology. Section A. Molecular Crystals and Liquid Crystals

Publication details, including instructions for authors and subscription information:
http://www.tandfonline.com/loi/gmcl19

Crystal Chemistry of Nanotubes Lattices

John E. Fischer [a], Agnes Claye [a] & Roland S. Lee [a]

[a] Department of Materials Science and Engineering and Laboratory for Research on the Structure of Matter, University of Pennsylvania, Philadelphia, PA, 19104, USA

Version of record first published: 24 Sep 2006

To cite this article: John E. Fischer, Agnes Claye & Roland S. Lee (2000): Crystal Chemistry of Nanotubes Lattices, Molecular Crystals and Liquid Crystals Science and Technology. Section A. Molecular Crystals and Liquid Crystals, 340:1, 737-742

To link to this article: http://dx.doi.org/10.1080/10587250008025556

Mol. Cryst. and Liq. Cryst., 2000, Vol. 340, pp. 737-742
Reprints available directly from the publisher
Photocopying permitted by license only

Crystal Chemistry of Nanotubes Lattices

JOHN E. FISCHER, AGNES CLAYE and ROLAND S. LEE

Department of Materials Science and Engineering and Laboratory for Research on the Structure of Matter, University of Pennsylvania, Philadelphia, PA 19104, USA

(Received June 22, 1999; In final form June 25, 1999)

X-ray diffraction profiles of pristine and hypothetical "intercalated" crystalline bundles of single-wall carbon nanotubes are computed and compared with experiment. The pristine case is complicated by finite size effects, tube diameter dispersion and the cylindrical form factor for uncorrelated tube rotations. Experimental profiles of "doped" samples are not in agreement with simulations based on 2-D ordered sublattices except at very low doping levels.

Keywords: nanotubes; diffraction; intercalation; doping

INTRODUCTION

Progress in intercalation science relies heavily on x-ray diffraction, particularly for graphite intercalation compounds, doped conjugated polymers and doped solid C_{60} [1]. The discovery that single-wall carbon nanotubes (SWNT) crystallize into bundles or "ropes" [2] prompted the idea that intercalation compounds could be prepared and similarly analyzed.

We first present diffraction profiles from pristine SWNT crystallites. The key points are that a) experimental peak positions cannot be directly indexed due to the combined effects of finite size and cylindrical form factor; b) variations in crystallite size lead to spurious peak shifts which mimic the effect of lattice dilation upon doping; and c) diameter dispersion can mean either segregation of different diameters into separate crystallites or crystallites containing tubes of different diameters. Then we address the problem of diffraction profiles from hypothetical intercalation superlattices, none of which agree with experiment.

PRISTINE SWNT DIFFRACTION

Since SWNT's are cylindrical, they naturally crystallize in a triangular lattice with 6-fold rotational symmetry, incompatible with the point symmetry of individual tubes except when n and m are molulo 6, e.g. (12,12), (6,0) etc. As a result, long-range order is frustrated and tube orientations are uncorrelated. This is analogous to the high temperature plastic crystal phase of fcc C_{60} for which the form factor is the spherical

(3-D) Bessel function of order zero [3], so we employed the cylindrical (2-D) analog to model the diffraction from finite crystallites of SWNT's. The results are shown in Figure 1. The combination of Bessel function form factor and finite coherence length shifts the observed peaks off the Bragg positions – the first peak ***underestimates*** **a** while the second one ***overestimates*** it. A correct analysis requires simultaneous optimization of **a** and tube diameter D.

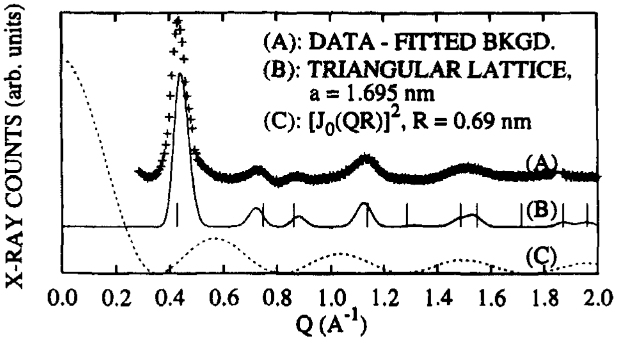

FIGURE 1. X-ray diffraction from pristine as-grown PLV material. (A) experimental profile with background subtracted; (B) simulated profile with **a** = 1.695 Å, 13.8 Å tube diameter and 100 Å coherence length; (C) the corresponding cylindrical form factor. Tick marks on (B) are the infinite crystal Bragg peak locations. From Ref. [2].

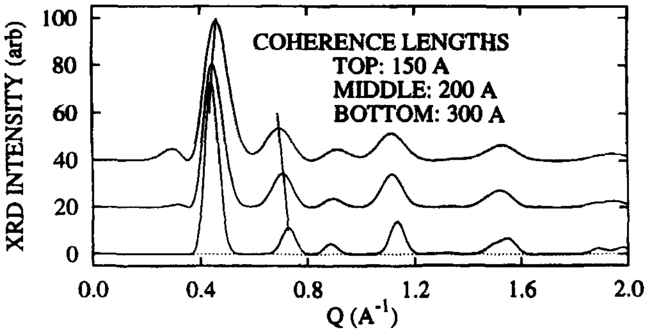

FIGURE 2. Effect of variable coherence length on observed peak positions, holding both D and **a** fixed.

Next we consider the effect of varying the coherence length, all other parameters being fixed. This effect can lead to incorrect interpretations of experiments designed to study the effect of growth conditions on average tube diameter [4,5] or lattice dilation associated with ordered dopant superlattices. In Figure 2 we display the simulated results of varying the inter-tube coherence length by a factor of 2, for a *fixed* lattice constant 16.76 Å and a *fixed* tube diameter 13.56 Å corresponding to (10,10). The ***apparent*** lattice constant derived from the first peak (without accounting for the Bessel function) decreases from 14.21 to 13.66 Å as the coherence length decreases from 300 to 150 Å. Including dispersity in tube diameter σ_D leads to a shift in the opposite direction [5]. Note also that the effect of variable coherence length on the second peak is opposite to that of the first one. Along with a and D, one must also optimize the coherence length and σ_D. Finally we point out that diameter dispersion σ_D can produce different effects according as the D's are random within a crystallite or phase separated into different crystallites. Crystallization *per se* implies a small σ_D within a crystallite, in which case the intensities $[S(Q)J_o(QD/2)]^2$ are additive. This appears to be the dominant effect in PLV material since the experimental profiles can be fit by a series of doublets [6]. On the other hand, diameter dispersion within a crystallite requires summing the weighted amplitudes $S(Q)J_o(QD/2)$ over the range σ_D and then squaring the sum. Assuming a constant VDW intertube spacing, σ_D must be accounted for both in S(Q) via the lattice constant and in J_o. For completeness one also needs to include dispersity in coherence lengths, i.e. bundles of different size as is commonly observed; and fluctuations in a (paracrystallinity) in the case of finite σ_D within a crystallite.

DOPED SWNT LATTICES

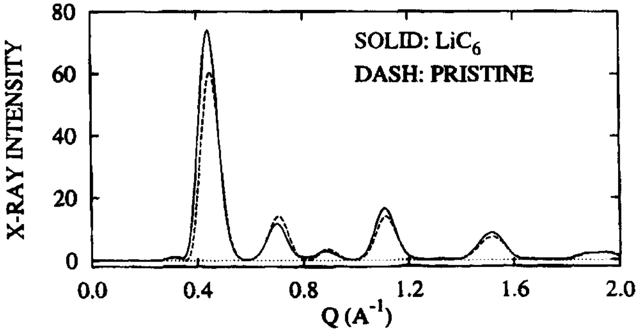

FIGURE 3. Simulated profiles of pristine and Li-intercalated SWNT lattices, assuming a, D and coherence length fixed at 16.95, 13.56 and 100 Å respectively.

The triangular lattice contains 2 trigonal interstitial channels per tube.

These are the most likely intercalation sites (assuming the tube ends are capped), and are large enough to accommodate as many as 3 chains each of small ions without inducing large lattice dilations. Assuming close packed ions along the tube axis, such a model would be consistent with a maximum doping level ~ LiC_6 as is observed [7]. This model also implies weak interactions between the dopant and the orientationally disordered SWNT. Figure 3 compares the simulated profiles of pristine and "LiC_6" lattices assuming no change in a, D or coherence length. Small shifts are apparent in the low-order reflections, due to the contribution of point Li atoms which partially cancels the effect of the SWNT Bessel function, *cf.* Figure 1. Note also that the low-order peaks increase slightly in intensity, due to the extra scattering power from the Li's.

In situ diffraction experiments have been performed using electrochemical Li intercalation [7], and the results are inconsistent with the simulation. Figure 4 shows that for very dilute doping the pristine lattice is progressively lost, with little or no shift or broadening. This suggests that the major structural effect of doping is to exfoliate the lattice into individual tubes. The lattice is not recovered by electrochemical de-intercalation, but is restored by high temperature vacuum annealing.

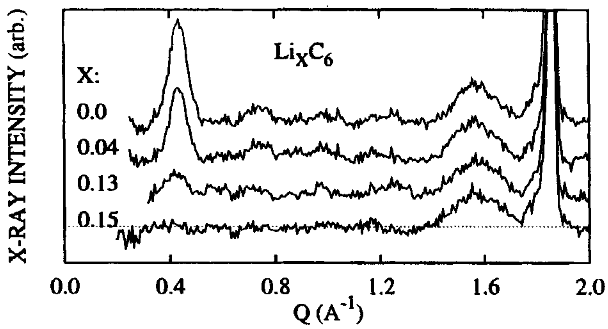

FIGURE 4. In situ XRD from Li-doped SWNT. Curves are labelled by Li concentration; note the progressive loss of intensity with increasing x, well below saturation. Broad peak at 1.6 Å^{-1} is from the electrolyte; the sharp one at 1.85 Å^{-1} is graphite impurity.

The channels are too small to accommodate large concentrations of K, Rb or Cs without dilating the lattice. Figure 5 is a simulation for precisely CsC_8 assuming a large lattice dilation, no change in D or coherence length, and strong Cs-SWNT interactions such that the Cs forms a 2 × 2 superlattice wrapped around each tube. The simulation bears no resemblance to the pristine case, and the peak intensity increases 7-fold upon doping. "RbC_8" should show similar but somewhat weaker effects, whereas experiment implies a small dilation (based on the first peak only) and a ~ 10-fold *decrease* in intensity [8]. This again suggests that the major doping effect is loss of crystallinity rather than formation of a coherent intercalation superlattice.

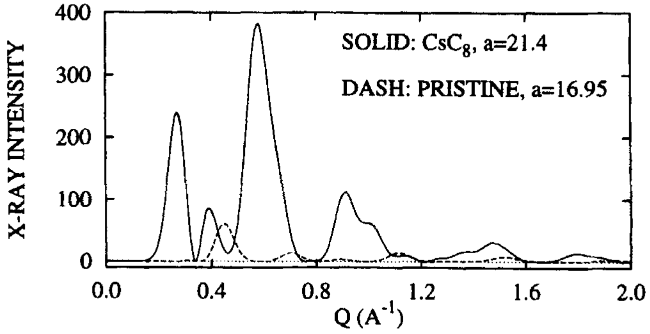

FIGURE 5. Simulated profiles of pristine and CsC_8 SWNT lattices. a is assumed to increase from 16.95 to 21.4 Å while D and coherence length are fixed at 13.56 and 100 Å respectively. Intensity scale same as Figure 3.

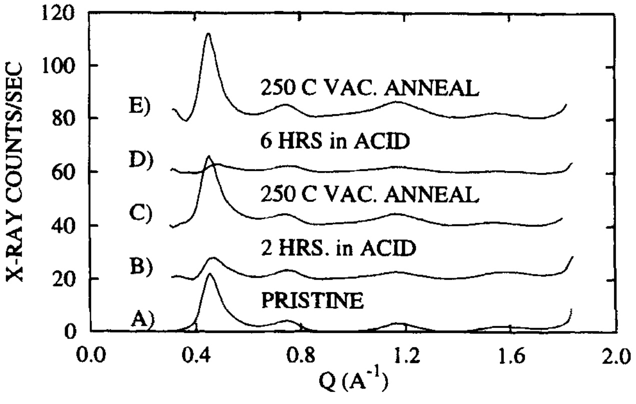

FIGURE 6. Experimental profiles of SWNT doped with HNO_3 and vacuum-annealed. Two complete cycles are shown, for 2 and 6 hours of doping.

Nanotubes are amphoteric; they can be oxidized or reduced, like graphite but unlike fullerenes. Acceptor compounds with halogens and acids have been reported [9-11]. Figure 6 shows our experimental results for 300 K immersion doping in 70% HNO_3. The bottom curve (A) is for the pristine sample. Curve (B) shows the result of 2 hour immersion; intensities are reduced, and the first peak shifts to ***higher*** Q, inconsistent with lattice dilation but consistent with a decrease in coherence length [5]. Using exactly the same doping procedure on different SWNT's, the UNC group observed a *downshift* of the first peak from 0.39 to 0.36 $Å^{-1}$. Curve (C) shows that the effect, whatever it is, is reversible. Curve (D) represents re-doping the same sample for 6 hours; now we observe a stronger reduction in intensity and a greater shift of the first peak to higher Q, consistent with additional loss of intertube coherence. This too is reversible, curve (E). As with the donors, the overall effect of acid doping appears to be a loss of crystallinity rather than formation of an intercalate superlattice. TEM observations bear this out [11].

CONCLUSIONS

Diffraction techniques can in principle give important structural information about pristine nanotubes, however a very careful analysis accounting for all the effects described herein is necessary in order to extract meaningful parameters. Doped SWNT lattices apparently become highly disordered except at very dilute concentrations, suggesting that the pristine lattice is only marginally stable and can be disrupted by very small lattice dilations and/or tube deformations. XRD has to date provided little useful information about doped SWNT; local probes such as TEM, AFM etc. may prove more useful.

Acknowledgments

Supported by Department of Energy Grant DEFG02-98ER45701 (JEF, RSL) and by the NSF MRSEC Grant DMR96-32598 (AC). We are grateful to the Rice University group for providing the SWNT material.

References

[1] J. E. Fischer and P. Bernier, *La Recherche*, **24**, 46 (1993).

[2] A. Thess *et al.*, *Science*, **273**, 483 (1996).

[3] J. E. Fischer and P. A. Heiney, *J. Phys. Chem. Solids*, **54**, 1725 (1993).

[4] S. Bandow *et al.*, *Phys. Rev. Lett.*, **80**, 3779 (1998).

[5] E. Anglaret, S. Rols and J.-L. Sauvajol, *Phys. Rev. Lett.*, **81**, 4780 (1998); S. Rols *et al.*, *Europhys. J.* in press.

[6] A. G. Rinzler *et al.*, *Appl. Phys. A*, **67**, 29 (1998).

[7] A. Claye and J. E. Fischer, this volume.

[8] L. Duclaux *et al.*, this volume; F. Beguin, private communication.

[9] R. S. Lee *et al.*, *Nature* **388**, 255 (1997).

[10] L. Grigorian *et al.*, *Phys. Rev. Lett.*, **80**, 5560 (1998).

[11] C. Bower *et al.*, *Chem. Phys. Lett.*, **285**, 230 (1998).